Cell PRESS
Open ACCESS
Cell Reports
Report

Differences in AMPA and Kainate Receptor Interactomes Facilitate Identification of AMPA Receptor Auxiliary Subunit GSG1L

Natalie F. Shanks,[1,3,7] Jeffrey N. Savas,[4,7] Tomohiko Maruo,[1,7] Ondrej Cais,[6] Atsushi Hirao,[5] Souichi Oe,[5] Anirvan Ghosh,[2] Yasuko Noda,[5] Ingo H. Greger,[6] John R. Yates III,[4] and Terunaga Nakagawa[1,*]
[1]Department of Chemistry and Biochemistry
[2]Division of Biology and Section of Neurobiology
[3]Neurosciences Graduate Program
University of California, San Diego, 9500 Gilman Drive, La Jolla, CA, 92093, USA
[4]Department of Chemical Physiology, The Scripps Research Institute, 10550 North Torrey Pines Road, SR11, La Jolla, CA 92037, USA
[5]Department of Anatomy, Jichi Medical University, 3311-1 Yakushiji, Shimotsuke-shi, Tochigi, 329-0498, Japan
[6]Neurobiology Division, MRC Laboratory of Molecular Biology, CB2 0QH Cambridge, UK
[7]These authors contributed equally to this work
*Correspondence: nakagawa@ucsd.edu
DOI 10.1016/j.celrep.2012.05.004

SUMMARY

AMPA receptor (AMPA-R) complexes consist of channel-forming subunits, GluA1-4, and auxiliary proteins, including TARPs, CNIHs, synDIG1, and CKAMP44, which can modulate AMPA-R function in specific ways. The combinatorial effects of four GluA subunits binding to various auxiliary subunits amplify the functional diversity of AMPA-Rs. The significance and magnitude of molecular diversity, however, remain elusive. To gain insight into the molecular complexity of AMPA and kainate receptors, we compared the proteins that copurify with each receptor type in the rat brain. This interactome study identified the majority of known interacting proteins and, more importantly, provides candidates for additional studies. We validate the claudin homolog GSG1L as a newly identified binding protein and unique modulator of AMPA-R gating, as determined by detailed molecular, cellular, electrophysiological, and biochemical experiments. GSG1L extends the functional variety of AMPA-R complexes, and further investigation of other candidates may reveal additional complexity of ionotropic glutamate receptor function.

INTRODUCTION

AMPA receptors (AMPA-Rs) and kainate receptors (KA-Rs) are members of the ionotropic glutamate receptor (iGluR) family, functioning as ligand-gated ion channels that mediate excitatory synaptic transmission and plasticity in the brain (Traynelis et al., 2010). Their functions are regulated by the composition of channel-forming core subunits, association with auxiliary proteins, phosphorylation, receptor trafficking, and interaction with cytoplasmic scaffolds (Jackson and Nicoll, 2011; Kim and Sheng, 2004; Shepherd and Huganir, 2007). Defining molecules that mediate receptor modulation is critical in understanding basic brain function and disease mechanisms. The molecular composition of AMPA-Rs and KA-Rs is diverse, and the complete landscape is currently unclear.

The iGluR's channel core is a tetrameric assembly of receptor subunits, GluA1-4 for AMPA-Rs and GluK1-5 for KA-Rs (Collingridge et al., 2009). Auxiliary transmembrane subunits bind to core iGluR subunits. They are found across species (Wang et al., 2008) and include stargazin/transmembrane AMPA-R regulatory proteins (stg/TARPs) (Chen et al., 2000; Tomita et al., 2003), SOL-1 (Zheng et al., 2004), cornichon2/3 (CNIH-2/3) (Schwenk et al., 2009), synDIG1 (Kalashnikova et al., 2010), and CKAMP44 (von Engelhardt et al., 2010) for AMPA-Rs and Neto1/2 (Zhang et al., 2009) for KA-Rs. The combinatorial effect of various auxiliary subunits binding to channel-forming core subunits extends the architectural and functional complexity of iGluRs in the brain (Farrant and Cull-Candy, 2010; Jackson and Nicoll, 2011).

iGluR complexes are extensively studied, yet new binding proteins are continuously reported. Biochemical hurdles in handling intact membrane proteins have been overcome for AMPA-Rs and KA-Rs by robust purification protocols (Nakagawa et al., 2005; Zhang et al., 2009). In combination with liquid chromatographic separations in line with tandem mass spectrometers, peptide analysis can identify nearly all proteins present in a low-complexity sample (Savas et al., 2011).

In this study, we wished to identify iGluR interactors that are less abundant or difficult to find. Specifically, we compared the interactomes of native AMPA-Rs and KA-Rs and identified an AMPA-R auxiliary subunit, GSG1L. GSG1L modifies AMPA-R channel function very differently from the known auxiliary modulators, revealing another functional repertoire of AMPA-Rs. This study provides a proof-of-principal for identifying novel interactors of iGluRs with the use of our interactome data. Our results

may also reveal previously unexpected molecular and functional diversity of iGluR complexes.

RESULTS

Identification of Candidate Proteins that Copurify with AMPA-Rs and KA-Rs in Rat Brain

We performed immunoaffinity purification of native AMPA-Rs and KA-Rs followed by shotgun liquid chromatography-tandem mass spectrometry (LC-MS/MS) protein analysis (AP-MS/MS). The copurifying proteins were directly analyzed by multidimensional protein identification technology (MudPIT) (Washburn et al., 2001). As a negative control, we performed a parallel purification with normal rabbit IgG. Any protein binding to IgG was excluded from analysis.

A summary and complete list of the proteins that copurify with brain AMPA-Rs and KA-Rs are shown in Tables 1 and S1, respectively. Our purification was highly enriched for the target proteins containing the epitopes of the antibodies used for affinity purification, as demonstrated by numerous spectrum counts (s.c.) and peptide counts (p.c.) for GluA2 (2526 s.c., 193 p.c.) and GluK2 (790 s.c., 88 p.c.). Nearly all known AMPA-R interacting membrane proteins, such as TARPs (stg/γ-2, γ-3, γ-4, γ-5, γ-7, and γ-8), CNIH-2/3, and CKAMP44, were identified in our AMPA-R preparation. Although we did not find synDIG1 itself, we identified homologs (Tables 1 and S1). Among the known auxiliary subunits, stg/TARPs were most abundantly detected, whereas fewer s.c.'s and p.c's were observed for the others. Furthermore, the known KA-R auxiliary subunits Neto1 and Neto2 were detected with KA-Rs (Tables 1 and S1). These results indicate that our purification was robust, and therefore, further investigation of the list may identify other interactors. Our results extend the current knowledge of the interactomes of AMPA-Rs and KA-Rs.

Predicted Protein GSG1L Is Expressed the Brain and Binds to AMPA-Rs

Among the candidates, we focused on the predicted protein GSG1L, a membrane protein specifically copurifying with AMPA-Rs (Figure 1A). It is a distant homolog of stg/TARPs belonging to the extended claudin family (Figure 1B). Furthermore, its peptide counts were comparable to known AMPA-R auxiliary subunits (Figure 1A and Table 1). GSG1L was reproducibly identified from rat brain (Tables 1 and S1) and also copurified with AMPA-Rs from human cortex (Figures S1A–S1C), indicative of evolutionary conservation of the interactome. Collectively, this evidence provided support for further investigation.

While it is in the claudin family, GSG1L is distinct from stg/TARPs, as there is a large evolutionary distance between GSG1L and stg/TARPs. The nearest family member of GSG1L is the product of germline-specific gene 1 (GSG1), whose transcript is specifically expressed in the germline and whose function is unknown (Tanaka et al., 1994).

Similar to claudins, the predicted topology of GSG1L has a cytoplasmic N terminus, four transmembrane segments, two extracellular loops, and a cytoplasmic C terminus (Figure 1C). Loop1 is ~50% longer in GSG1L than in TARPs. The extracellular and cytoplasmic domains of GSG1L are not conserved with stg/TARPs (Figure S1D). These regions are responsible for modulating AMPA-R function in stg/TARPs (Tomita et al., 2005); therefore, GSG1L may potentially have a unique modulatory function.

GSG1L was annotated as a predicted protein in the rat genome. Its protein existence was unknown and two alternatively spliced transcripts were predicted (GenBank entries XP_002725730.1 and XP_574558.2; predicted molecular weights 26 and 36 kDa, respectively). The shorter variant lacks the first 102 amino acids, including the first transmembrane domain. We first created three polyclonal antibodies against different epitopes of the predicted GSG1L protein (Figure S1D). The first epitope, Lp1, is present only in the product of the longer spliced variant. When we purified native AMPA-Rs from rat brain tissue and examined GSG1L by Western blot, all three antibodies detected a band at the molecular weight of 43 kDa, consistent with the long isoform (Figures 1D1 and 1D2). These results establish that GSG1L is a protein expressed in rat brain and copurifies with native AMPA-Rs.

GSG1L Interacts Specifically with AMPA-R Subunits In Vitro

To reconstitute the interaction in nonneuronal cells, we transfected a plasmid encoding hemagglutinin (HA)-tagged GSG1L into stable human embryonic kidney (HEK) cell lines that express either GluA2 or GluK2 and immunoprecipitated the HA-GSG1L by using an anti-HA antibody. GluA2 coimmunoprecipitated with GSG1L, whereas GluK2 did not (Figures 1E1 and 1E2). Under the same conditions, the known KA-R auxiliary subunit Neto2 specifically interacted with GluK2 but not with GluA2. Conversely, the specific interaction of GSG1L with GluA2 and not with GluK2 was also observed when the immunoprecipitation was performed with the use of antibodies directed against each glutamate receptor subunit (Figures S2A1 and 2). Furthermore, GSG1L and GluA2 partially colocalize near the plasma membrane when coexpressed in a stable HEK cell line with the use of a DOX-inducible expression system (Figure 1F). Similar results were obtained when the two proteins were coexpressed through transient transfection (Figure S2B). GluA1 also forms a complex with GSG1L, as determined by coimmunoprecipitation experiments (Figure 1G). These observations establish the physical interaction between GSG1L and AMPA-R subunits.

Functional Interaction of GSG1L with AMPA-Rs

Next, we investigated functional interactions between GSG1L and AMPA-Rs. Transfection of GSG1L into a stable HEK cell line that expresses GluA2 increased the surface expression of GluA2 as compared to transfecting EGFP. In fact, GSG1L increased the surface expression of GluA2 as efficiently as stg (Figures 2A and 2B), indicating that surface expression of AMPA-Rs is positively modulated by GSG1L.

A functional interaction was also detected by a cell-death assay (Sans et al., 2003; Shanks et al., 2010) (Figure S3). For this purpose, we created stable TetON HEK cell lines that express GluA2 in a DOX-dependent fashion and constitutively express GSG1L or stg (Figure S3A). Cell death was observed after GluA2 expression was induced by DOX in the cell line constitutively expressing stg or GSG1L. Cytotoxicity was blocked by the AMPA-R antagonist NBQX and was not detected

Table 1. Comparison of AMPA-R and KA-R Interactomes by Mass Spectrometry

IPI	GluA2 Spec,Pep (%AA)	GluA2 Norm	GluK2 Spec,Pep (%AA)	GluK2 Norm	Common Name
Known Primary Interactors					
IPI00780113.1	2526, 193 (71.3)•	1.0000	17, 11 (17.2)•	0.0215	GluA2
IPI00324555.2	876, 129 (60.4)•	0.3468	6, 3 (5.1)	0.0076	GluA1
IPI00231095.1	873, 121 (56.5)•	0.3456	6, 4 (4.8)	0.0076	GluA3
IPI00195445.1	585, 91 (48.7)•	0.2316	3, 2 (2.4)	0.0038	GluA4
IPI00207460.1	212, 26 (34.0)•	0.0839	0, 0 (0.0)	0.0000	TARP gamma-3
IPI00201313.4	193, 28 (39.6)•	0.0764	0, 0 (0.0)	0.0000	TARP gamma-2
IPI00207426.1	162, 28 (36.8)•	0.0641	5, 2 (8.3)	0.0063	TARP gamma-8
IPI00207431.1	78, 13 (32.4)•	0.0309	0, 0 (0.0)	0.0000	TARP gamma-4
IPI00214444.1	11, 4 (23.3)•	0.0044	0, 0 (0.0)	0.0000	TARP gamma-7
IPI00207430.1	3, 2 (6.9)	0.0012	0, 0 (0.0)	0.0000	TARP gamma-5
IPI00366152.2	18, 6 (13.1)•	0.0071	0, 0 (0.0)	0.0000	CNIH-2
IPI00358957.3	11, 4 (9.0)	0.0044	0, 0 (0.0)	0.0000	CNIH-3
IPI00956073.1	*147, 13 (26.2)*	*0.0582*	*0, 0 (0.0)*	*0.0000*	*Shisa-9/CKAMP-44*
IPI00566635.2	255, 61 (65.1)•	0.1010	28, 10 (16.0)•	0.0354	PSD-95
IPI00777470.1	80, 31 (40.7)•	0.0317	208, 62 (62.7)•	0.2633	SAP-97
IPI00650099.1	53, 21 (27.9)•	0.0210	140, 48 (42.4)•	0.1772	PSD-93
IPI00568474.1	28, 14 (19.6)•	0.0111	27, 11 (10.0)	0.0342	SAP-102
IPI00208830.1	2, 2 (3.0)	0.0008	0, 0 (0.0)	0.0000	Grip1
IPI00409970.1	0, 0 (0.0)	0.0000	2, 2 (6.3)	0.0025	Grip2
IPI00204506.1	5, 5 (6.7)•	0.0020	42, 20 (22.8)•	0.0532	protein4.1
IPI00210635.2	16, 13 (19.5)•	0.0063	32, 20 (36.0)•	0.0405	NSF
IPI00471901.3	11, 6 (8.4)•	0.0044	10, 6 (10.2)•	0.0127	AP-2 alpha2
IPI00389753.1	6, 6 (9.3)•	0.0024	10, 6 (7.6)	0.0127	AP-2 beta
IPI00203346.4	5, 4 (6.3)•	0.0020	8, 6 (10.1)•	0.0101	AP-2 alpha1
IPI00196530.1	4, 3 (5.7)	0.0016	5, 4 (11.5)•	0.0063	AP-2 mu
IPI00198371.1	2, 2 (14.1)	0.0008	4, 3 (24.6)	0.0051	AP-2 sigma
IPI00324708.1	0, 0 (0.0)	0.0000	790, 88 (47.8)•	1.0000	GluK2
IPI00207006.1	0, 0 (0.0)	0.0000	190, 52 (48.0)•	0.2405	GluK5
IPI00231400.2	0, 0 (0.0)	0.0000	187, 36 (29.1)•	0.2367	GluK1
IPI00231277.4	2, 2 (2.2)•	0.0008	686, 77 (45.4)•	0.8684	GluK3
IPI00326553.1	0, 0 (0.0)	0.0000	105, 32 (34.5)•	0.1329	GluK4
IPI00359373.3	0, 0 (0.0)	0.0000	125, 37 (59.7)•	0.1582	Neto2
IPI00367046.2	*0, 0 (0.0)*	*0.0000*	*37, 14 (38.3)*	*0.0468*	*Neto1*
IPI00370061.1	0, 0 (0.0)	0.0000	19, 14 (22.8)•	0.0241	Kelch
Candidate Interactors					
IPI00763858.2	0, 0 (0.0)	0.0000	9, 5 (13.3)•	0.0114	MAGUK p55
IPI00365736.3	14, 11 (12.0)•	0.0055	5, 5 (6.1)	0.0063	Liprin alpha 3
IPI00392157.3	0, 0 (0.0)	0.0000	14, 13 (13.9)•	0.0177	Liprin alpha 4
IPI00388795.3	11, 8 (12.6)	0.0044	94, 32 (36.6)	0.1190	CASK
IPI00214300.1	0, 0 (0.0)	0.0000	37, 12 (42.6)	0.0342	Lin 7
IPI00367477.1	56, 21 (29.8)•	0.0222	0, 0 (0.0)	0.0000	NGL-3 (LRRC 4b)
IPI00207958.1	11, 7 (11.4)•	0.0044	0, 0 (0.0)	0.0000	NGL-1 (LRRC 4c)
IPI00360822.3	4, 3 (5.1)	0.0016	0, 0 (0.0)	0.0000	LRRTM3
IPI00454354.1	3, 3 (4.3)	0.0012	8, 6 (5.3)•	0.0101	LRRC 7
IPI00206020.1	3, 3 (19.2)	0.0012	5, 3 (11.1)	0.0063	LRRC 59
IPI00372074.1	2, 2 (4.0)	0.0008	0, 0 (0.0)	0.0000	LRRC 8
IPI00359172.2	0, 0 (0.0)	0.0000	3, 2 (5.9)	0.0038	LRRC 47

Table 1. *Continued*

IPI	GluA2 Spec,Pep (%AA)	GluA2 Norm	GluK2 Spec,Pep (%AA)	GluK2 Norm	Common Name
IPI00367715.3	2, 2 (3.9)	0.0008	0, 0 (0.0)	0.0000	FLRT-2
IPI00829463.1	10, 8 (7.8)•	0.0040	10, 7 (6.5)•	0.0127	Nrxn-1
IPI00195792.3	10, 7 (6.8)•	0.0004	6, 6 (7.8)•	0.0076	Nrxn-2
IPI00829491.1	5, 4 (6.1)	0.0020	4, 2 (2.7)•	0.0051	Nrxn-3
IPI00325649.1	3, 2 (4.9)	0.0012	0, 0 (0.0)	0.0000	Nlgn-2
IPI00325804.1	0, 0 (0.0)	0.0000	5, 2 (3.3)•	0.0063	Nlgn-3
IPI00764645.1	30, 15 (23.2)•	0.0119	0, 0 (0.0)	0.0000	EphB2
IPI00189428.1	4, 3 (5.5)	0.0016	0, 0 (0.0)	0.0000	EphB1
IPI00569433.1	3, 3 (6.7)•	0.0012	0, 0 (0.0)	0.0000	EphA4
IPI00230960.1	2, 2 (4.8)•	0.0008	0, 0 (0.0)	0.0000	EphA5
IPI00365395.2	2, 2 (13.4)	0.0008	0, 0 (0.0)	0.0000	EphrinB2
IPI00411236.1	10, 7 (8.1)•	0.0040	13, 8 (9.3)•	0.0165	Latrophilin 1
IPI00561212.4	9, 8 (9.2)•	0.0036	0, 0 (0.0)	0.0000	Latrophilin 3
IPI00568123.2	4, 3 (4.3)	0.0016	0, 0 (0.0)	0.0000	Latrophilin 2
IPI00568245.2	0, 0 (0.0)	0.0000	480, 136 (57.5)•	0.6076	myosin 18
IPI00193933.3	3, 3 (6.0)	0.0012	0, 0 (0.0)	0.0000	DHHC5
IPI00357941.4	7, 7 (5.8)	0.0028	0, 0 (0.0)	0.0000	RTPT delta
IPI00231945.4	3, 2 (3.3)	0.0012	0, 0 (0.0)	0.0000	RTPT
IPI00565098.2	30, 13 (25.8)•	0.0119	0, 0 (0.0)	0.0000	GSG1L
IPI00939232.1	*2, 2 (5.1)*	*0.0008*	*0, 0 (0.0)*	*0.0000*	*Shisa-6*
IPI00214724.3	4,20 (12.1)•	0.0016	0, 0 (0.0)	0.0000	PPRT 1
IPI00366048.3	38, 10 (38.1)	0.0150	0, 0 (0.0)	0.0000	PPRT 2
IPI00207495.3	0, 0 (0.0)	0.0000	32, 13 (24.5)•	0.0405	pentraxin-2 (Narp)
IPI00192125.1	0, 0 (0.0)	0.0000	58, 19 (29.9)•	0.0734	pentraxin-1
IPI00212317.1	0, 0 (0.0)	0.0000	69, 16 (36.6)•	0.0873	pentraxin receptor
IPI00206558.4	19, 9 (15.1)•	0.0075	0, 0 (0.0)	0.0000	Olfm1
IPI00337161.1	5, 3 (8.7)	0.0020	0, 0 (0.0)	0.0000	Olfm3

Known primary interactors and candidate interactors are listed by common name and IPI number. The spectrum count (Spec), peptide count (Pep), and coverage percentage (%AA) identified by LC-MS/MS as well as the normalized (Norm) abundance of the protein relative to the immunoprecipitated target protein are listed for proteins in both the GluA2 (A2) and GluK2 (K2) preparations. The current annotated rat protein database does not provide complete representation of the proteins in the rat genome. Thus, to identify Shisa-6, Shisa-9, and Neto1 (shown in italics), we searched against a concatenated database consisting of the human-mouse-rat protein databases. References of known and candidate interactors are provided in the Extended Discussion. Black dots represent proteins that were also found in a smaller-scale duplication experiment.
(See Table S1 for full lists.)

in the absence of stg or GSG1L (Figure S3C). Glutamate in the media thus triggered the cell death by activating AMPA-Rs whose function was enhanced by stg or GSG1L.

GSG1L Profoundly Slows AMPA-R Recovery from the Desensitized State

TARPs, which are distantly related to GSG1L (Figures 1B and 1C), alter AMPA-R gating kinetics (Tomita et al., 2005). Specifically, deactivation and desensitization rates are slowed by both type I and type II TARPs (with the exception of γ-5; Jackson and Nicoll, 2011), and recovery from desensitization is accelerated (Priel et al., 2005).

To examine GSG1L's potential function, we coexpressed it with GluA2-Q (flip) in HEK 293T cells. Channel kinetics were assessed by ultrafast agonist application to outside-out membrane patches. In response to a sustained L-glutamate pulse (10 mM for 100 ms), the GSG1L AMPA-R complex desensitized approximately 2-fold more slowly (data were fitted with two exponentials; weighted τ_{des} = 4.76 ± 0.16 ms, n = 27, versus 9.50 ± 0.21 ms, n = 10; $p < 0.0001$; t test) (Figures 2C and 2D [left bar graph]). This difference is largely due to an increase in the relative amplitude of the slow component of the decay (A_{slow} = 10 ± 2% and 47 ± 5% without and with GSG1L, respectively) and, to a lesser extent, to an increase in the time constants of the individual components (τ_{fast} and τ_{slow} shift from 4.09 ± 0.13 ms and 11.58 ± 0.85 ms to 4.86 ± 0.40 ms and 15.18 ± 0.82 ms, respectively). In addition, the 20%–80% rise time of these responses was also slightly slower with GSG1L (0.23 ± 0.02 ms versus 0.19 ± 0.01 ms; $p < 0.05$; t test).

A more dramatic effect surfaced when recovery from desensitization was analyzed via a two-pulse protocol. Whereas GluA2 recovered with a time constant of 18 ± 1 ms (n = 10), the presence of GSG1L slowed recovery by ~10-fold (τ_{rec} = 196 ± 28 ms, n = 6; $p < 0.005$, Mann-Whitney U test) (Figures 2D [right

Cell PRESS
Open ACCESS

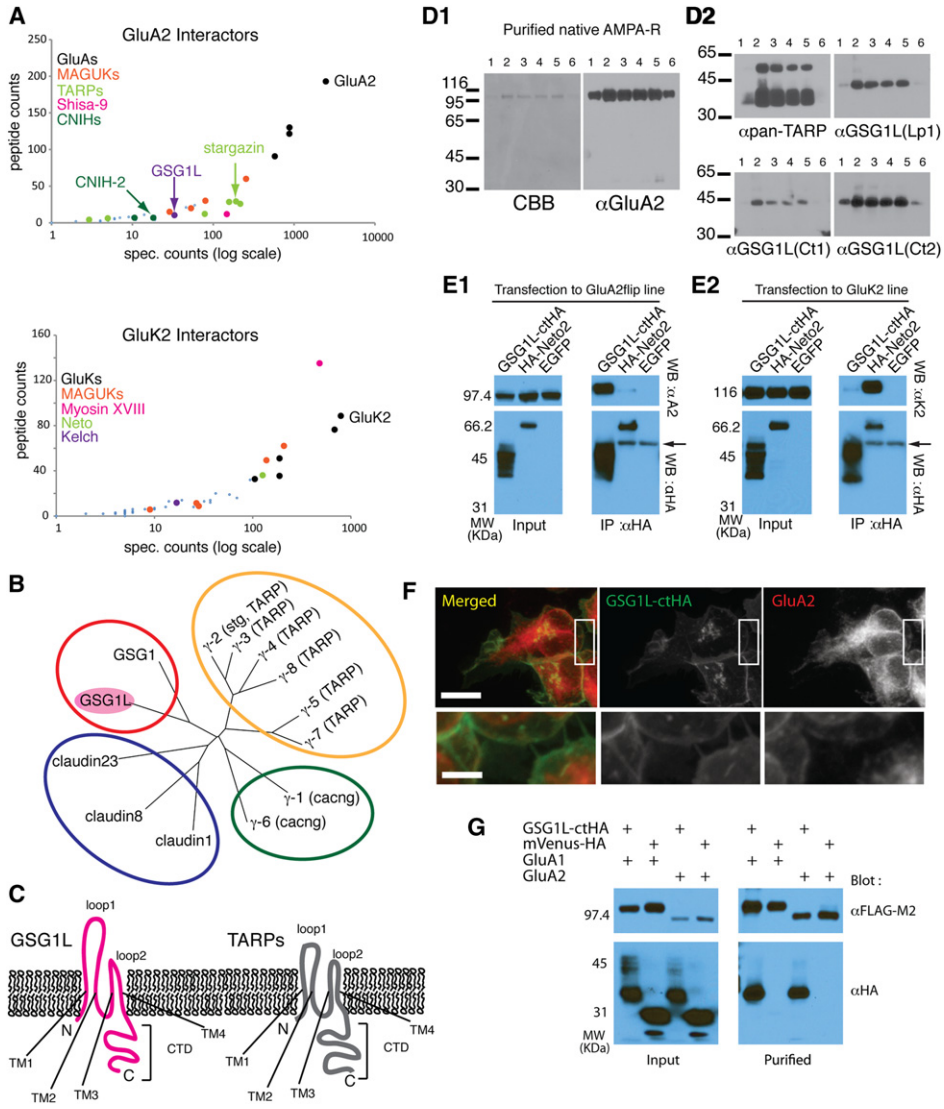

Figure 1. Comparative Interactomes of Native AMPA-R and KA-R Identify GSG1L as an AMPA-R-Interacting Protein

(A) Graphical representation of proteins identified as interacting with GluA2 (top) and GluK2 (bottom). Each dot represents a protein identified by mass spectrometry. The-*y* axis is the number of peptides (log scale) and the *x* axis represents the number of spectra in which the identified proteins were found. The black dots are the bait protein receptor subunits. Other known interactor protein families are highlighted by different color dots (see legend). The larger dots indicate known interactors, whereas the smaller dots indicate potential candidates. Note the location of GSG1L between data points for stg and CNIH-2.

(B) Phylogenic tree of representative proteins in claudin family constructed using neighbor-joining algorithm in CLUSTALW. The red, yellow, green, and blue circles represents families of GSG, stg/TARPs, gamma subunit of calcium channels, and conventional claudins.

(C) Topology of GSG1L (magenta) and TARPs (gray) relative to the membrane. TM1-4 = transmembrane domain 1-4, loop1-2 = extracellular loop 1-2, CTD = C-terminal domain. GSG1L loop1 is ~50% longer compared to TARPs.

(D) Left: CBB staining of purified native AMPA-Rs. Fractions 1–6 are consecutive elutions from the antibody column using antigen peptide. Right: Western blots of same fractions probed with anti-GluA2CT (αGluA2). Molecular weight markers are on the left (kDa) (D1). The duplicated membranes resolving the fractions in D1 were probed with anti-pan-TARP and anti-GSG1L (three different antibodies; Lp1, Ct1, and Ct2, each recognizing different epitopes) antibodies. GSG1L copurifies with AMPA-Rs from rat brain (D2).

(E) Western blots of the input and immunoprecipitate (IP). (E1) Stable HEK cell line expressing GluA2flip was transfected with plasmids expressing GSG1LctHA (ctHA indicates an HA tag at the C terminus), HA-Neto2, and EGFP. Cellular lysates were IPed using anti-HA antibody. The Western blot was probed with antibodies indicated on right. The arrow indicates the IgG derived from the antibody used for IP. (E2) An experiment similar to that illustrated in panel E1 was conducted, but with the use of a stable HEK cell line expressing GluK2.

(F) Confocal images of HEK cells coexpressing GSG1LctHA and GluA2. Scale bar = 10μm (upper) and 2.5 μm (lower).

(G) HEK cells were transfected with plasmids expressing the proteins indicated at the top of each lane. FLAG tagged GluA1 and 2 subunits were affinity purified using FLAG beads. The bound protein was eluted using FLAG epitope peptide. Western blots were conducted using the indicated antibodies. mVenus variant of EYFP was used as a negative control.

(See Figures S1 and S2 as well.)

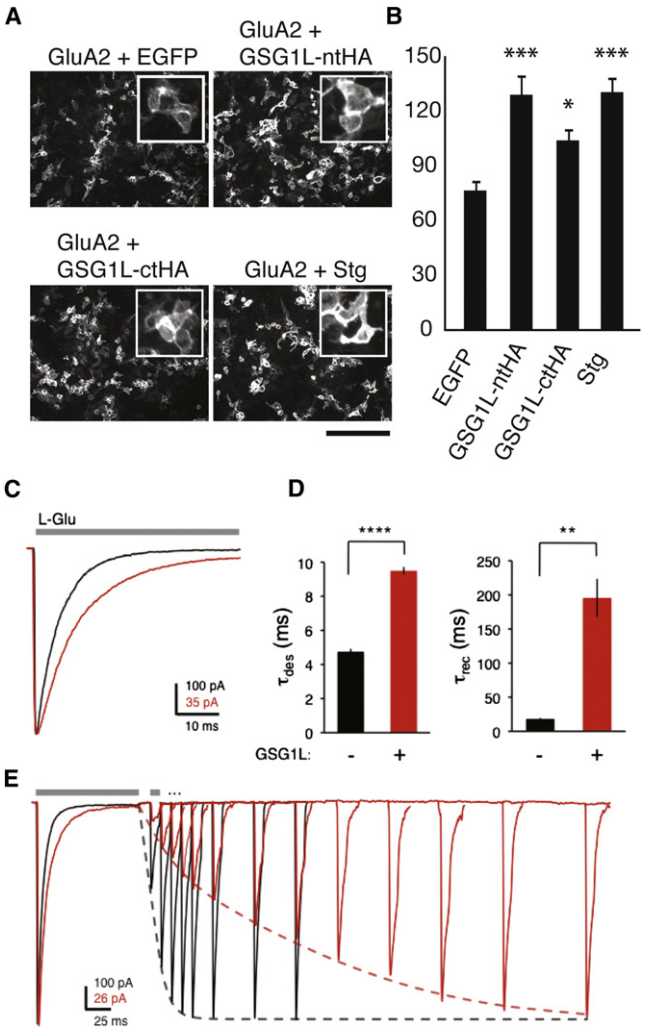

Figure 2. Functional Modulation of AMPA-R by GSG1L

(A) Cell surface staining of GluA2 in HEK cells cotransfected with plasmids expressing the proteins indicated above each image. Scale bar = 200μm. Insets are representative enlarged views.

(B) Bar graph summarizing the quantification obtained from C. *** and * indicate, respectively, $p < 0.0003$ and $p < 0.0166$ against control experiments using EGFP according to Bonferroni's corrected student t test. The vertical axis represents arbitrary units of fluorescence intensity.

(C) Example current responses of outside-out patches from HEK293T cells expressing GluA2-Q(flip) without (black) or with (red) GSG1L to a 100 ms application of 10 mM L-Glu (holding potential −60 mV). Data were fitted with two exponentials. The weighted τ_{des} of the traces presented here is 5.55 ms and 10.70 ms in the absence and presence of GSG1L, respectively.

(D) Summary bar graph for the time constants of desensitization (left) and recovery from desensitization (right). Data are presented as mean ± SEM. ****$p < 0.0001$ (t test); **$p < 0.005$ (Mann-Whitney U test).

(E) Representative current traces of outside-out patches from HEK293T cells expressing GluA2-Q(flip) demonstrating recovery from desensitization in the presence (red) or absence (black) of GSG1L. The paired-pulse protocol consisted of a 100 ms pulse of 10 mM L-Glu followed by a 10 ms pulse in an interval increasing by 10 ms (only selected sweeps are shown). Traces are peak-scaled to the amplitude of the first pulse. Dashed lines indicate the single-exponential fits of the recovery (τ_{rec} = 15 ms and 140 ms for GluA2-Q(flip) without and with GSG1L, respectively; summarized in D).

(See Figure S3 as well.)

bar graph] and 2E). Interestingly, despite the structural similarity between GSG1L and TARPs (Figures 1C and S1D), this recovery phenotype is in fact opposite of what has been described for TARPs acting on GluA1 but parallels the effect of CKAMP44, a structurally unrelated Cys-knot protein (von Engelhardt et al., 2010). However, GSG1L and CKAMP44 have opposite effects on modulation of desensitization. Therefore, GSG1L is an auxiliary factor that confers newly identified gating properties, further increasing the AMPA-R functional repertoire. Collectively, these data establish the existence of a functional interaction between GSG1L and AMPA-Rs.

Localization of GSG1L in Neurons

The in situ hybridization data in the Allen Brain Atlas indicate GSG1L RNA signals in the hippocampus, striatum, and cortex (Lein et al., 2007). Consistently, GSG1L immunoreactivity was detected in CA3 pyramidal neurons and partially colocalized with excitatory synaptic marker PSD-95 (Figure 3A). Despite our efforts, none of the antibodies generated could detect endogenous GSG1L in dissociated cultured cortical or hippocampal neurons. However, our antibodies could detect GSG1L when it was moderately overexpressed in cultured neurons. We speculate that our antibodies do not have affinity high enough to detect the endogenous proteins in cultured neurons and/or that the expression level of GSG1L in culture is lower than that in brain tissue.

To gain insight into the distribution of GSG1L in neurons, we analyzed the subcellular localization of GSG1L transfected into cortical neurons. To detect GSG1L at the neuronal cell surface, we used a GSG1L construct with an HA epitope tag in the extracellular loop1 (see Experimental Procedures). Consistent with the physical and functional interactions described above, surface GSG1L colocalized with endogenous AMPA-R subunits GluA1 and GluA2 (Figures 3B and 3C). The punctate subcellular distribution of surface GSG1L also colocalized with the excitatory synaptic marker PSD-95 (Figure 3D). These results suggest that GSG1L exists at the excitatory synapses in neurons where AMPA-Rs are present.

DISCUSSION

Interactome Data Identify Candidates Forming the iGluR Complex

By searching through the data set for membrane proteins that specifically copurify with AMPA-Rs and homologs of known interactors, we reduced the list of candidates significantly. After taking into account the s.c.'s and p.c.'s, we thought it likely that GSG1L is a biologically significant AMPA-R interactor (Figure 1A). Validation of the interaction is the rate-limiting step, requiring multiple experimental approaches. Additional investigations of other candidates from our data are expected to validate additional components of AMPA-R and KA-R complexes (see Extended Discussion).

GSG1L Is an AMPA-R-Specific Auxiliary Subunit

The GSG1L gene is implicated as playing roles in the nervous system. Its transcript level increases during synapse formation

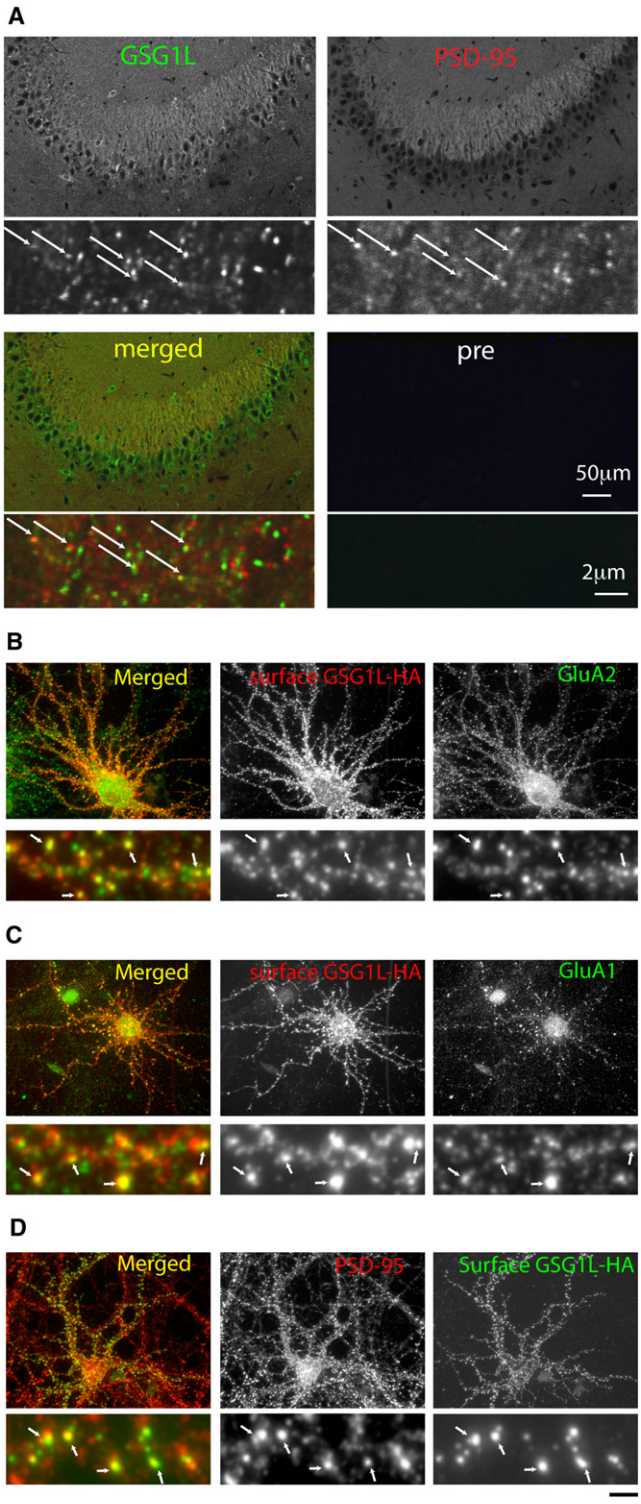

Figure 3. Localization of GSG1L in Neurons

(A) Confocal images of sections of rat hippocampus stained with anti-GSG1L antibody Lp1 and preimmune serum control (pre). Sections were double stained with PSD-95, Scale bar = 50 μm (upper) and 2 μm (lower). Arrows indicate colocalizing puncta.

(B) Confocal images of dissociated cortical neurons overexpressing HA tagged GSG1L. The HA tag is in the extracellular loop enabling surface labeling. GSG1L expressed at the cell surface (red) and colocalizes with GluA2 (green). Upper panels; low magnification. Lower panels; enlarged view of the dendrite. The single scale bar corresponds to 20 μm for the upper and 2 μm for the lower panels. Arrows indicate colocalizing puncta.

(C) A similar experiment as B was conducted using anti-GluA1 antibody. GSG1L (red) expressed at the cell surface colocalizes with GluA1 (green).

(D) A similar experiment as B was conducted using anti-PSD-95 antibody. GSG1L (green) expressed at the cell surface partially colocalizes with PSD-95 (red).

(Brusés, 2010; Lai et al., 2011) and decreases in Huntington's disease (Becanovic et al., 2010).

Both GSG1L and TARPs are members of the tetraspanin superfamily, with GSG1L belonging to the evolutionarily distant claudin family. The extracellular loop1 of GSG1L is least conserved (19% homology and 6.25% identity) when compared with stg/TARPs and is substantially longer (~50%) (Figures 1C and S1D). Because this loop is essential for ion channel modulation by stg/TARPs (Menuz et al., 2008; Tomita et al., 2005), divergence in AMPA-R channel modulation may be due to mechanistic differences in how the loop interacts with AMPA-Rs. Indeed, whereas TARPs speed recovery from the desensitized state, GSG1L slows this parameter, mimicking the structurally unrelated Cys-knot protein CKAMP44 (von Engelhardt et al., 2010). Given that desensitization and recovery from the desensitized state have an impact on high-frequency transmission (Arai and Lynch, 1998), synaptic AMPA-Rs associated with GSG1L are not expected to follow high-frequency trains with great fidelity. Additional experiments are necessary to define the mechanisms of binding and functional modulation between GSG1L and TARPs with AMPA-Rs.

Although stg/TARPs increase surface expression of AMPA-Rs in HEK cells, there was no change in the amplitude of the AMPA-R mediated current in neurons overexpressing stg (Kessels et al., 2009). Increased surface expression of AMPA-Rs by GSG1L in HEK cells may not warrant such modulation occurring in neurons. Additional experiments are needed to investigate the differences and similarities between GSG1L and stg/TARPs in the modulation of synaptic physiology.

GSG1L is structurally related to stg/TARPs yet confers completely different function to AMPA-Rs; therefore, investigating homologs of known interactors may reveal more about the functional repertoire of AMPA-Rs. In fact, we identified many related proteins of known interactors (Tables 1 and S1). For example, the LRRC and Shisa families of proteins are related to known AMPA-R interactors LRRTM2 and CKAMP44 (de Wit et al., 2009; Pei and Grishin, 2012). Similarly, PRRT 1 (NG5 and synDIG4), and pancortin-3 (Olfm1) are shown to copurify with AMPA-Rs (von Engelhardt et al., 2010). Our study extends the interactome by identifying homologs such as PRRT 2 and Olfm3.

Given the large number of auxiliary subunits identified for AMPA-Rs, questions regarding their distribution in the brain and their stoichiometry remain. Different auxiliary subunits simultaneously interact with a single tetramer of GluA subunits (Kato et al., 2010). AMPA-R complexes with different molecular composition may be used during spatiotemporal regulation in

specific neurons and synapses. Exactly how this extensive diversity contributes to the activity of neural circuits and behavior remains unclear and is an important question that still needs to be addressed.

EXPERIMENTAL PROCEDURES

Purification of AMPA and KA-Rs from Brain

Purification of AMPA-Rs and KA-Rs from rat brain was performed according to previous protocols used for single-particle EM study of native AMPA-Rs (Nakagawa et al., 2005). All experiments involving animal tissues were performed according to procedures approved by the Institutional Animal Care and Use Committee at UCSD.

Mass Spectrometry

Tryptic digests of resuspended TCA precipitates were subjected to Multidimensional Protein Identification Technology (MudPIT) (Washburn et al., 2001). Low-resolution LTQ mass spectrometers were utilized for rat samples, and high-resolution LTQ Orbitrap Velos were used for human samples. The. RAW and parameter files will be publicly available at http://fields.scripps.edu/published/iGluR upon publication.

Plasmid DNA Construction

Rat GSG1L cDNA was synthesized (Genscript) on the basis of GenBank entry XP_574558.2 and tagged with HA or FLAG. The expression plasmids pTREt, pIRESmcherry (Clontech), and pBOSS (Shanks et al., 2010) were used.

Coimmunoprecipitation Experiments

HEK cells were transfected with various expression plasmids, and the cellular lysates were prepared from detergent extracts. Anti-HA, -FLAG, -GluA2CT, and -GluK2CT antibodies were used for immunoprecipitation.

Generation of Stable TetON HEK Cell Lines

Cell lines were generated with the use of previously described methods (Farina et al., 2011; Shanks et al., 2010).

Surface Labeling of GluA2 in HEK Cells

TetON HEK cells (Clontech) were transfected with appropriate pTREt plasmids in order to coexpress GluA2 together with GSG1L, stg, or EGFP. Surface GluA2 was live labeled with an anti-GluA2-NTD antibody (1:100, Chemicon MAB397).

Neuron Transfection and Surface Labeling

Embryonic day 18 cortical culture and surface labeling were performed as previously described (Shanks et al., 2010; Sala et al., 2003) with slight modifications.

Electrophysiology

Voltage-clamp recordings were performed on outside-out patches from HEK 293T cells as described previously (Rossmann et al., 2011).

Immunohistochemistry

A 6-week-old rat (male) was anesthetized and fixed by perfusion with the use of 4% paraformaldehyde in normal rat Ringer solution; 40 μm cryostat brain sections were used.

SUPPLEMENTAL INFORMATION

Supplemental Information includes Extended Results, an Extended Discussion, Extended Experimental Procedures, three figures, and one table and can be found with this article online at doi:10.1016/j.celrep.2012.05.004.

LICENSING INFORMATION

ACKNOWLEDGMENTS

This work was supported by the John Merck Fund and NIH grant R01 HD061543 to T.N. J.N.S. is supported by NRSA fellowship 1F32AG039127. J.R.Y. is supported by R01 MH067880 and P41 RR011823. Human brain cortex was obtained through the National Disease Research Interchange (NDRI); Researcher: Yates (code YAJ2); TSRI: IRB-11-5719.

Received: February 1, 2012
Revised: April 2, 2012
Accepted: May 7, 2012
Published online: May 23, 2012

REFERENCES

Arai, A., and Lynch, G. (1998). AMPA receptor desensitization modulates synaptic responses induced by repetitive afferent stimulation in hippocampal slices. Brain Res. *799*, 235–242.

Becanovic, K., Pouladi, M.A., Lim, R.S., Kuhn, A., Pavlidis, P., Luthi-Carter, R., Hayden, M.R., and Leavitt, B.R. (2010). Transcriptional changes in Huntington disease identified using genome-wide expression profiling and cross-platform analysis. Hum. Mol. Genet. *19*, 1438–1452.

Brusés, J.L. (2010). Identification of gene transcripts expressed by postsynaptic neurons during synapse formation encoding cell surface proteins with presumptive synaptogenic activity. Synapse *64*, 47–60.

Chen, L., Chetkovich, D.M., Petralia, R.S., Sweeney, N.T., Kawasaki, Y., Wenthold, R.J., Bredt, D.S., and Nicoll, R.A. (2000). Stargazin regulates synaptic targeting of AMPA receptors by two distinct mechanisms. Nature *408*, 936–943.

Collingridge, G.L., Olsen, R.W., Peters, J., and Spedding, M. (2009). A nomenclature for ligand-gated ion channels. Neuropharmacology *56*, 2–5.

de Wit, J., Sylwestrak, E., O'Sullivan, M.L., Otto, S., Tiglio, K., Savas, J.N., Yates, J.R., 3rd, Comoletti, D., Taylor, P., and Ghosh, A. (2009). LRRTM2 interacts with Neurexin1 and regulates excitatory synapse formation. Neuron *64*, 799–806.

Farina, A.N., Blain, K.Y., Maruo, T., Kwiatkowski, W., Choe, S., and Nakagawa, T. (2011). Separation of domain contacts is required for heterotetrameric assembly of functional NMDA receptors. J. Neurosci. *31*, 3565–3579.

Farrant, M., and Cull-Candy, S.G. (2010). Neuroscience. AMPA receptors—another twist? Science *327*, 1463–1465.

Jackson, A.C., and Nicoll, R.A. (2011). The expanding social network of ionotropic glutamate receptors: TARPs and other transmembrane auxiliary subunits. Neuron *70*, 178–199.

Kalashnikova, E., Lorca, R.A., Kaur, I., Barisone, G.A., Li, B., Ishimaru, T., Trimmer, J.S., Mohapatra, D.P., and Díaz, E. (2010). SynDIG1: an activity-regulated, AMPA- receptor-interacting transmembrane protein that regulates excitatory synapse development. Neuron *65*, 80–93.

Kato, A.S., Gill, M.B., Ho, M.T., Yu, H., Tu, Y., Siuda, E.R., Wang, H., Qian, Y.W., Nisenbaum, E.S., Tomita, S., and Bredt, D.S. (2010). Hippocampal AMPA receptor gating controlled by both TARP and cornichon proteins. Neuron *68*, 1082–1096.

Kessels, H.W., Kopec, C.D., Klein, M.E., and Malinow, R. (2009). Roles of stargazin and phosphorylation in the control of AMPA receptor subcellular distribution. Nat. Neurosci. *12*, 888–896.

Kim, E., and Sheng, M. (2004). PDZ domain proteins of synapses. Nat. Rev. Neurosci. *5*, 771–781.

Lai, H.C., Klisch, T.J., Roberts, R., Zoghbi, H.Y., and Johnson, J.E. (2011). In vivo neuronal subtype-specific targets of Atoh1 (Math1) in dorsal spinal cord. J. Neurosci. *31*, 10859–10871.

Lein, E.S., Hawrylycz, M.J., Ao, N., Ayres, M., Bensinger, A., Bernard, A., Boe, A.F., Boguski, M.S., Brockway, K.S., Byrnes, E.J., et al. (2007). Genome-wide atlas of gene expression in the adult mouse brain. Nature *445*, 168–176.

Menuz, K., O'Brien, J.L., Karmizadegan, S., Bredt, D.S., and Nicoll, R.A. (2008). TARP redundancy is critical for maintaining AMPA receptor function. J. Neurosci. *28*, 8740–8746.

Nakagawa, T., Cheng, Y., Ramm, E., Sheng, M., and Walz, T. (2005). Structure and different conformational states of native AMPA receptor complexes. Nature *433*, 545–549.

Pei, J., and Grishin, N.V. (2012). Unexpected diversity in Shisa-like proteins suggests the importance of their roles as transmembrane adaptors. Cell. Signal. *24*, 758–769.

Priel, A., Kolleker, A., Ayalon, G., Gillor, M., Osten, P., and Stern-Bach, Y. (2005). Stargazin reduces desensitization and slows deactivation of the AMPA-type glutamate receptors. J. Neurosci. *25*, 2682–2686.

Rossmann, M., Sukumaran, M., Penn, A.C., Veprintsev, D.B., Babu, M.M., and Greger, I.H. (2011). Subunit-selective N-terminal domain associations organize the formation of AMPA receptor heteromers. EMBO J. *30*, 959–971.

Sala, C., Futai, K., Yamamoto, K., Worley, P.F., Hayashi, Y., and Sheng, M. (2003). Inhibition of dendritic spine morphogenesis and synaptic transmission by activity-inducible protein Homer1a. J. Neurosci. *23*, 6327–6337.

Sans, N., Prybylowski, K., Petralia, R.S., Chang, K., Wang, Y.X., Racca, C., Vicini, S., and Wenthold, R.J. (2003). NMDA receptor trafficking through an interaction between PDZ proteins and the exocyst complex. Nat. Cell Biol. *5*, 520–530.

Savas, J.N., Stein, B.D., Wu, C.C., and Yates, J.R., 3rd. (2011). Mass spectrometry accelerates membrane protein analysis. Trends Biochem. Sci. *36*, 388–396.

Schwenk, J., Harmel, N., Zolles, G., Bildl, W., Kulik, A., Heimrich, B., Chisaka, O., Jonas, P., Schulte, U., Fakler, B., and Klöcker, N. (2009). Functional proteomics identify cornichon proteins as auxiliary subunits of AMPA receptors. Science *323*, 1313–1319.

Shanks, N.F., Maruo, T., Farina, A.N., Ellisman, M.H., and Nakagawa, T. (2010). Contribution of the global subunit structure and stargazin on the maturation of AMPA receptors. J. Neurosci. *30*, 2728–2740.

Shepherd, J.D., and Huganir, R.L. (2007). The cell biology of synaptic plasticity: AMPA receptor trafficking. Annu. Rev. Cell Dev. Biol. *23*, 613–643.

Tanaka, H., Yoshimura, Y., Nishina, Y., Nozaki, M., Nojima, H., and Nishimune, Y. (1994). Isolation and characterization of cDNA clones specifically expressed in testicular germ cells. FEBS Lett. *355*, 4–10.

Tomita, S., Chen, L., Kawasaki, Y., Petralia, R.S., Wenthold, R.J., Nicoll, R.A., and Bredt, D.S. (2003). Functional studies and distribution define a family of transmembrane AMPA receptor regulatory proteins. J. Cell Biol. *161*, 805–816.

Tomita, S., Adesnik, H., Sekiguchi, M., Zhang, W., Wada, K., Howe, J.R., Nicoll, R.A., and Bredt, D.S. (2005). Stargazin modulates AMPA receptor gating and trafficking by distinct domains. Nature *435*, 1052–1058.

Traynelis, S.F., Wollmuth, L.P., McBain, C.J., Menniti, F.S., Vance, K.M., Ogden, K.K., Hansen, K.B., Yuan, H., Myers, S.J., Dingledine, R., and Sibley, D. (2010). Glutamate receptor ion channels: structure, regulation, and function. Pharmacol. Rev. *62*, 405–496.

von Engelhardt, J., Mack, V., Sprengel, R., Kavenstock, N., Li, K.W., Stern-Bach, Y., Smit, A.B., Seeburg, P.H., and Monyer, H. (2010). CKAMP44: a brain-specific protein attenuating short-term synaptic plasticity in the dentate gyrus. Science *327*, 1518–1522.

Wang, R., Walker, C.S., Brockie, P.J., Francis, M.M., Mellem, J.E., Madsen, D.M., and Maricq, A.V. (2008). Evolutionary conserved role for TARPs in the gating of glutamate receptors and tuning of synaptic function. Neuron *59*, 997–1008.

Washburn, M.P., Wolters, D., and Yates, J.R., 3rd. (2001). Large-scale analysis of the yeast proteome by multidimensional protein identification technology. Nat. Biotechnol. *19*, 242–247.

Zhang, W., St-Gelais, F., Grabner, C.P., Trinidad, J.C., Sumioka, A., Morimoto-Tomita, M., Kim, K.S., Straub, C., Burlingame, A.L., Howe, J.R., and Tomita, S. (2009). A transmembrane accessory subunit that modulates kainate-type glutamate receptors. Neuron *61*, 385–396.

Zheng, Y., Mellem, J.E., Brockie, P.J., Madsen, D.M., and Maricq, A.V. (2004). SOL-1 is a CUB-domain protein required for GLR-1 glutamate receptor function in C. elegans. Nature *427*, 451–457.